PROCEEDINGS OF SPIE

SPIEDigitalLibrary.org/conference-proceedings-of-spie

Mid-IR emission characteristics of low-phonon erbium-doped ternary chloride-based single crystals

Brown, E., Fleischman, Z., Hawrami, R., Ariesanti, E., Burger, A., et al.

E. Brown, Z. D. Fleischman, R. Hawrami, E. Ariesanti, A. Burger, U. Hömmerich, S. B. Trivedi, M. Dubinskii, "Mid-IR emission characteristics of low-phonon erbium-doped ternary chloride-based single crystals," Proc. SPIE 11682, Optical Components and Materials XVIII, 116820R (5 March 2021); doi: 10.1117/12.2579430



Event: SPIE OPTO, 2021, Online Only

Mid-IR emission characteristics of low-phonon erbium-doped ternary chloride-based single crystals

E. Brown*a, Z. D. Fleischman^a, R. Hawrami^b, E. Ariesanti^b, A. Burger^b, U. Hömmerich^c, S.B. Trivedi^d, and M. Dubinskii^a

^aUS Army Research Laboratory, ATTN FCDD-RLS-RL, 2800 Powder Mill Rd, Adelphi, MD, USA 20783-1138; ^bDept. of Life and Physical Sciences, Fisk University, Nashville, TN, USA 37208-1002; ^c Dept. of Physics, Hampton University, Hampton, VA, USA 23668-0105; ^dBrimrose Corporation of America, Sparks Glencoe, MD, USA 21152-2300

ABSTRACT

The mid-infrared fluorescence properties of erbium (Er) doped low-phonon ternary chloride-based crystals (KPb₂Cl₅, Cs₂HfCl₆, CsPbCl₃, CsCdCl₃) have been investigated. All crystals were grown by vertical Bridgman technique. Following optical excitations at 805 nm and 660 nm, all Er³⁺ doped chlorides exhibited infrared emissions at ~2750, ~3500, and ~4500 nm at room temperature. The mid-infrared emission at 4500 nm originating from the ${}^4I_{9/2} \rightarrow {}^4I_{11/2}$ transition showed long emission lifetime values of ~7.8 ms and ~11.6 ms for Er³⁺ doped Cs₂HfCl₆ and CsCdCl₃ crystals, respectively. In comparison, Er³⁺ doped KPb₂Cl₅ and CsPbCl₃ demonstrated shorter lifetimes of ~3 ms and ~1.8 ms, respectively. The temperature dependence of the ${}^4I_{9/2}$ decay times was performed for Er³⁺ doped CsPbCl₃ and CsCdCl₃ crystals. We observed that the fluorescence lifetimes were nearly independent of the temperature, indicating a negligibly small non-radiative decay rate through multiphonon relaxation, as predicted by the energy gap law for low phonon energy hosts. The room temperature stimulated emission cross-sections for the ${}^4I_{9/2} \rightarrow {}^4I_{11/2}$ transition were determined to be in a range of ~0.14-0.54 x 10⁻²⁰ cm² for the studied Er doped chloride crystals.

Keywords: rare earth ions, erbium, mid-infrared, chlorides, solid-state lasers,

1. INTRODUCTION

Solid-state lasers operating in the mid-IR wavelength region (3-5 μ m) have attracted much interest for their various applications in remote sensing of bio-chemical agents, free-space communications, and medical procedures [1-12]. The development of mid-IR solid-state lasers based on traditional oxide crystals is hindered by large non-radiative decay rates through multi-phonon relaxation (MPR). The challenge is that when we are dealing with small energy gap for mid-IR transition, it is known that MPR is a competitive nonradiative process that can reduce the emission efficiency. According to well-known energy-gap law, the rate of nonradiative decay through multiphonon- relaxation (W_{MPR}) between rare-earth energy levels is expressed by [2]:

$$W_{MPR} = Be^{-\beta\Delta E} [1 - e^{-(\hbar\omega/kT)}]^{-p}$$
(1)

where ΔE is the energy spacing of the transition, T is the temperature, $\hbar \omega$ is the maximum phonon energy of the host material, p is the number of phonons needed to bridge the energy gap, and B and β are host dependent parameters. The rule of thumb is the more phonons required to bridge the gap between the upper and lower laser levels, the less likely it will be for non-radiative decay to occur (Fig. 1). Therefore, the way to mitigate that is to choose host materials with low-maximum phonon energies so that it takes more phonons to bridge the energy gap. Recently, there has been renewed interest in ternary chlorides as laser hosts due to their low phonon energies and compatibility with trivalent rare earth dopants [3-8]. Many rare-earth (RE) ions have rich energy level schemes offering potential emission transitions in the 3-5 μ m spectral region. Laser operation in the mid-IR spectral regions has been reported from RE doped halides and sulfides, with maximum phonon energies of 200 to 350 cm⁻¹ [3-12].

*eiei.brown.civ@mail.mil; phone 1 301 394-2293; fax 1 301 394-0310

Optical Components and Materials XVIII, edited by Shibin Jiang, Michel J. F. Digonnet, Proc. of SPIE Vol. 11682, 116820R · © 2021 SPIE · CCC code: 0277-786X/21/\$21 doi: 10.1117/12.2579430

Potassium lead chloride, KPb₂Cl₅ has been well-studied and has shown laser demonstrations from several RE ions in the near-IR and mid-IR spectral regions [3,4]. Cs₂HfCl₆, CsPbCl₃, and CsCdCl₃ have maximum phonon energies of ~250-375 cm⁻¹ [13,14], which make them particularly attractive as RE hosts for mid-IR laser applications. Most of their attention so far has been towards studies on optoelectronic, solar cell device, and scintillator applications since they are known for their optical and luminescent properties as well as scintillation characteristics [15-17]. To the best of our knowledge, there are no reports on mid-IR studies from Erbium doped in these three ternary chlorides. Virey et al. [18] reported the room temperature mid-IR (3-5 μm) fluorescence properties of several RE ions doped into CsCdBr₃. In this work, preliminary spectroscopic results of the mid-IR emission properties of Er³⁺ doped low-phonon ternary chloride-based crystals (Cs₂HfCl₆, CsPbCl₃, CsCdCl₃) are presented. These results were compared to previous and ongoing investigations of Er³⁺ doped KPb₂Cl₅, for which laser operation has already been demonstrated.

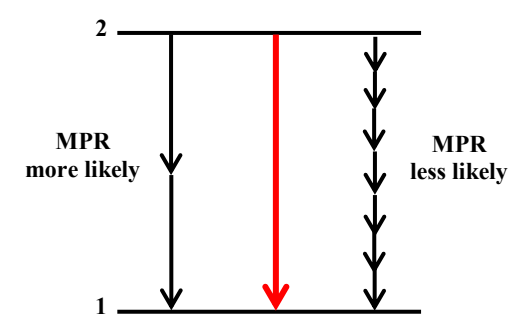


Figure 1. A schematic illustration of multiphonon-relaxation according to energy-gap law.

2. EXPERIMENTAL CONSIDERATIONS

KPb₂Cl₅ (KPC) is a monoclinic crystal with a transparency range of 0.3-20 μm [3,4]. The rest of the chloride crystals studied here, Cs₂HfCl₆ (CHC), CsPbCl₃ (CPC), and CsCdCl₃ (CCC) crystallize in the cubic perovskite structure [15-17]. They all have low maximum phonon energies between 200 and 400 cm⁻¹ [3,4,13,14], a wide band gap, and a wide transparency range. The physical properties of all chloride crystals, including their corresponding maximum phonon energies are listed in Table 1. KPC is considered non-hygroscopic whereas CHC, CPC and CCC have a varying degree of moisture sensitivity. The Er3+ doped CHC and CPC crystals were grown at Fisk University using the vertical Bridgman technique. For the growth of Cs₂HfCl₆:ErCl₃ (3%) and CsPbCl₃:ErCl₃ (3%), stoichiometric amounts of starting materials HfCl₄ + 2CsCl, ErCl₃ and CsCl + PbCl₂, ErCl₃, respectively were loaded into a baked ampoule. The materials in the ampoule endured dehydration and the ampoule was sealed under a high vacuum ≤1 x 10⁻⁵ Torr. The ampoules were subsequently placed into a two-zone furnace and the growth rate was 3-4 mm/hour. More details of the purification and crystal growth process were described elsewhere [15]. Er³⁺ doped KPC and CCC crystals were grown at Hampton University using Bridgman technique. KPC and CCC were synthesized using a stoichiometric ratio of commercial starting materials of PbCl₂ (5N) + KCl (5N) and CdCl₂ (4N) + CsCl (5N), respectively. The synthesized KPC was then purified through 5-10 unidirectional translations in a horizontal zone-refinement system. Er:CCC was synthesized from commercial raw materials without further purification. The purified KPC and synthesized CCC were then loaded with 1-2 wt.% of ErCl₃. The synthesized Er:KPC and Er:CCC crystals were subsequently grown by a twozone crystal growth furnace and the growth speed of 1-3 mm/hr was used. Details of the material preparation and crystal growth process were expressed elsewhere [19]. The Er³⁺ concentrations in the studied samples were ranging between 1.5 and 2 x 10²⁰ cm⁻³. Figure 2 shows pictures of the as-grown boules and cut pieces of the studied Er³⁺ doped chloride crystals. All crystals were successfully doped with erbium as can be seen (Fig. 2) by a quick test for the tell-tale green emission from UV excitation. Despite the slow cooling rate, some cracking of the crystals occurred during the cooling process. Crack-free samples with good optical quality were selected and polished for spectroscopic measurements. It was noted that Er:KPC showed light pink color and was stable under normal atmospheric conditions whereas Er:CCC exhibited no inherent color and its moisture sensitivity was very low. Er:CHC showed some hygroscopicity for which they were required to be stored within a vial of mineral oil. Slight yellow-greenish coloration and translucent character was noticed for Er:CPC which became slightly milky after being exposed to the atmosphere for a few hours. X-ray diffraction measurements verified the crystal structure of all of the studied chloride crystals.

Room temperature transmission and absorption spectra were recorded using a Cary 6000i UV-Vis-NIR spectrophotometer and a Nicolet 6700 Fourier-transform infrared spectrometer. Mid-IR fluorescence spectra were recorded after excitation with either a continuous-wave Spectra-Physics Tsunami Ti:Sapphire laser (800-805 nm) or using the output of a pulsed (10 ns pulses, 10 Hz) Nd:YAG pumped Optical Parametric Oscillator (OPO) system. A Princeton Instruments Acton Spectra-Pro 0.15 m monochromator (λ_{blaze}: 4 μm, 150 grooves/mm) was used to collect the mid-IR emission spectra. The emission signal was recorded by an Infrared Associates liquid-nitrogen-cooled InSb detector in conjunction with a Stanford Research Systems SR830 dual-phase lock-in amplifier. Fluorescence decay measurements were carried out using the above-mentioned OPO system. The emission decay transients were recorded with a LabView-driven National Instruments data acquisition system. For temperature dependence emission studies, the sample was mounted on the cold finger of a two-stage closed-cycle helium refrigerator.

Table 1. Physical characteristics of all studied Er³⁺ doped ternary chloride crystals. * The maximum phonon energy of CHC listed in the table was determined from our own Raman spectroscopic measurement.

Property	KPb ₂ Cl ₅ (KPC)	2 3		Cs ₂ HfCl ₆ (CHC)	
Crystal structure	Monoclinic	Cubic perovskite	Cubic perovskite	Cubic	
Transparency Range (μm)	0.3 - 20	0.4 - 15	0.3 - 15	0.2 - 15	
Melting point (°C)	434	610	553	820	
Density (g/cm ³)	4.63	3.94	3.86	3.86	
Band gap (eV)	~ 3.77	~ 3.0	~ 4.76	~ 6.0	
Refractive index	~1.95 [3,4]	~1.91 [20]	~1.72 [21]	~1.4 [15]	
Maximal phonon energy (cm ⁻¹)	203 [3,4]	~ 375 [13]	~ 252 [14]	~ 333*	
Robustness	Non- hygroscopic	Low moisture sensitivity	Low moisture sensitivity	Hygroscopic	

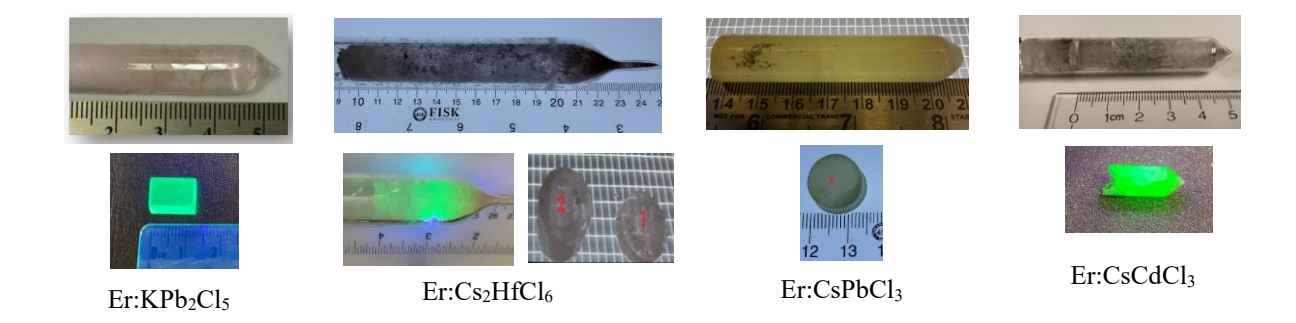


Figure 2. Pictures of as-grown boules and cut pieces of Er:KPC, Er:CHC, Er:CPC, and Er:CCC crystals. The characteristic Er³⁺ green emission was excited with a UV source and observed from all samples except Er: CPC due to its smaller bandgap.

3. RESULTS AND DISCUSSION

Figure 3 shows the room temperature transmission and absorption spectra of Er^{3+} doped KPC, CHC, CPC, and CCC crystals. The IR transmissions of Er:KPC and Er:CCC crystals were over ~60 % while the Er:CHC and Er:CPC displayed much lower transmittance (Fig. 3 (a)). In all cases, the transmittance reduced considerably in the visible wavelengths due to background losses. As can be seen in Fig. 3 (a), KPC and CPC exhibit a band edge at ~330 nm and 400 nm, respectively. While CCC and CHC each present wider bandgap with a band edge at 260 nm and 200 nm, respectively. Figure 3 (b) depicts the absorption spectra of all crystals, which were corrected for background absorption due to Fresnel and other parasitic loss effects. As indicated in Fig. 3 (c), each Er^{3+} absorption band originates from the $^{4}I_{15/2}$ ground state and terminates at a higher excited state. We observed strong absorption bands in the visible and weaker bands in the IR region. It is well known that Er^{3+} has absorption bands at ~800 nm ($^{4}I_{15/2} \rightarrow ^{4}I_{9/2}$) and ~980 nm ($^{4}I_{15/2} \rightarrow ^{4}I_{11/2}$), which are of great significance for laser diode pumping.

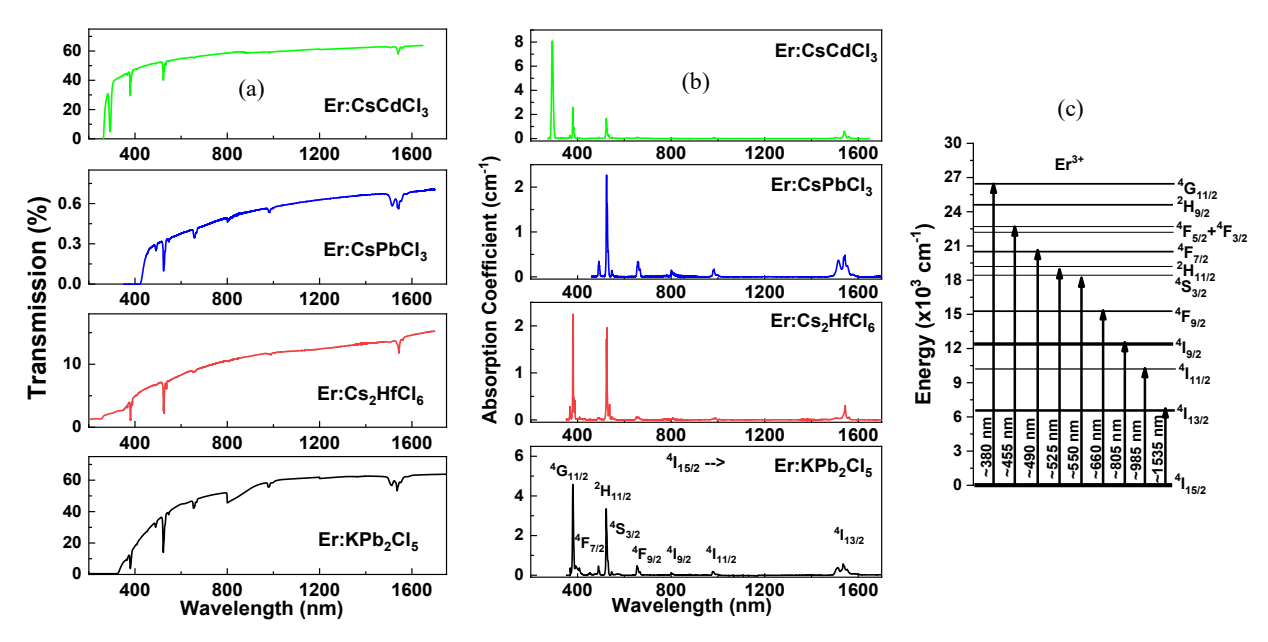


Figure 3. Room temperature (a) transmission and (b) absorption spectra of all Er^{3+} doped studied chloride crystals. (c) An energy level diagram indicating the corresponding absorption lines from the ground state ${}^{4}I_{15/2}$.

Figure 4 (a) - (c) illustrates the room temperature mid-IR emission bands of Er3+ doped chloride crystals in the wavelength ranges 2400 - 3100 nm, 3000 - 4100 nm, and 4000 - 5100 nm, which arise from ${}^{4}I_{11/2} \rightarrow {}^{4}I_{13/2}$, ${}^{4}F_{9/2} \rightarrow {}^{4}I_{9/2}$, and ${}^4I_{9/2} \rightarrow {}^4I_{11/2}$ transitions, respectively. Excitation of the upper levels of these transitions was attained using ~805 nm, which directly populated the ${}^{4}I_{9/2}$ level, and subsequently the ${}^{4}I_{11/2}$ level through radiative and nonradiative transitions. The ⁴F_{9/2} level was excited using 660 nm excitation. A schematic diagram of the relevant Er³⁺ energy levels indicating the excitation transitions and observed emission lines is depicted in Fig. 4 (d). Broad mid-IR emissions centered at ~2750 nm (FWHM: ~80 - 130 nm), ~3600 nm (FWHM: ~160 - 350 nm), and ~4500 nm (FWHM: ~175 - 330 nm) were observed. Virey et al. reported mid-IR fluorescence bands for ~2.7, ~3.5, and ~4.5 µm for Er³⁺ doped CsCdBr₃ [18] and appeared to observe similar emission features as in the studied Er3+ doped CsCdCl3 crystal. The emission lifetimes of the first four excited states of all investigated Er3+ doped ternary chloride crystals are presented in Table 2. In this work, the primary energy level of interest is ⁴I_{9/2}, which is the upper level of 4.5 µm transition, and for which all crystals showed emission lifetimes in millisecond range. Figure 5 (a) depicts the decay transients monitored at ~4500 nm emission at room temperature for all four crystals. It can be noted that the longest emission lifetimes was observed from Er³⁺ doped CHC and CCC crystals, which showed 7.8 ms and 11.6 ms, respectively. While Er:KPC and Er:CPC demonstrated decent lifetimes of 3.2 ms and 1.8 ms, respectively. These long lifetimes have sparked heightened interest for further exploration on temperature dependent decay dynamics. Hence, measurements of fluorescence decay times of the 4I_{9/2} excited state for Er doped CPC and CCC crystals were carried out for temperatures ranging from 10 K to room

temperature. As can be seen in Fig. 5 (b), the nearly temperature independent fluorescence lifetimes is consistent with a negligibly small non-radiative decay rate for the ${}^{4}I_{9/2}$ excited state of Er^{3+} as anticipated by the energy-gap law.

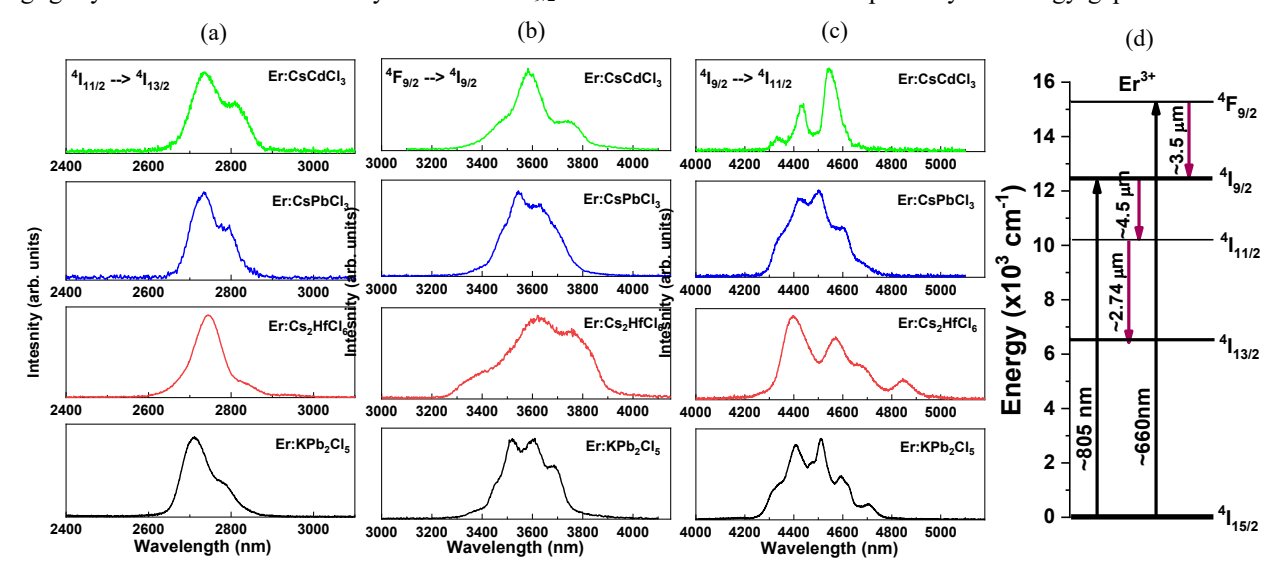


Figure 4. Room temperature infrared emission spectra of (a) ${}^4I_{11/2} \rightarrow {}^4I_{13/2}$ (b) ${}^4F_{9/2} \rightarrow {}^4I_{9/2}$ and (c) ${}^4I_{9/2} \rightarrow {}^4I_{11/2}$ transitions in Er³⁺ doped ternary chloride crystals. (d) The partial energy level diagram of Er³⁺ ions indicating the excitation wavelength and corresponding emission transitions.

Table 2. Measured (experimental) lifetime values of the first four excited states for all investigated Er³⁺ doped ternary chloride crystals.

Er ³⁺ Energy Levels	ΔE (cm ⁻¹)	Er:KPb ₂ Cl ₅ (ħω~203 cm ⁻¹) τ _{expt}	Er:Cs ₂ HfCl ₆ (ħω~333 cm ⁻¹) τ _{expt}	Er:CsPbCl ₃ (ħω~375 cm ⁻¹) τ _{expt}	Er:CsCdCl ₃ (ħω~252 cm ⁻¹) τ _{expt}
⁴ I _{13/2}	~ 6520	6.7 ms	10.2 ms	4.2 ms	12.3 ms
$^{4}I_{11/2}$	~ 3640	4.2 ms	4.0 ms	2.6 ms	12.5 ms
⁴ I _{9/2}	~ 2225	3.2 ms	7.8 ms	1.8 ms	11.6 ms
⁴ F _{9/2}	~ 2760	0.4 ms	1.1 ms	0.3 ms	2.1 ms

The emission quantum efficiency (η_{QE}) can be estimated from the ratio of the experimental (τ_{expt}) and radiative lifetimes (τ_{rad}): $\eta_{QE} = \tau_{expt}/\tau_{rad}$. The quantum yield of a specific transition, η_{ij} can be expressed by $\eta_{ij} = \beta_{ij}$ η_{QE} , where β_{ij} is the branching ratio, defined as the fraction of photons specifically emitted on that transition compared to all photons emitted from that level. Radiative lifetimes and branching ratios of RE transitions are frequently obtained from the Judd-Ofelt (J-O) Theory [2]. For the investigated Er:CPC and Er:CCC crystals, the maximum lifetime values, from temperature dependent emission lifetimes between 10 K and room temperature, were assumed as radiative lifetimes of ${}^4I_{9/2} \rightarrow {}^4I_{11/2}$ transition. The spectroscopic parameters from J-O analysis for Er³⁺ doped KPC are available in literature [22] since it has been well studied. The branching ratio of the ${}^4I_{9/2} \rightarrow {}^4I_{11/2}$ transition was reported to be ~1.3 % for the Er:KPC crystal. Since J-O analysis had not been performed yet, the stated value of 1.3% from Er:KPC was appropriated for the other crystals in a crude estimate of their respective quantum yield. This assumption was justified because the branching ratio for this small energy gap is expected to be typically ~1 to ~2 % [3-6,9,22]. The quantum yields of ${}^4I_{9/2} \rightarrow {}^4I_{11/2}$ transition were estimated to be ~1.3 % and ~1.2 % for Er:CPC and Er:CCC, respectively, which compare favorably to that of Er:KPC (~1.1 %) crystal. The room temperature, radiative lifetimes, and quantum efficiencies of the 4.5 µm transition (${}^4I_{9/2} \rightarrow {}^4I_{11/2}$) are listed in Table 3.

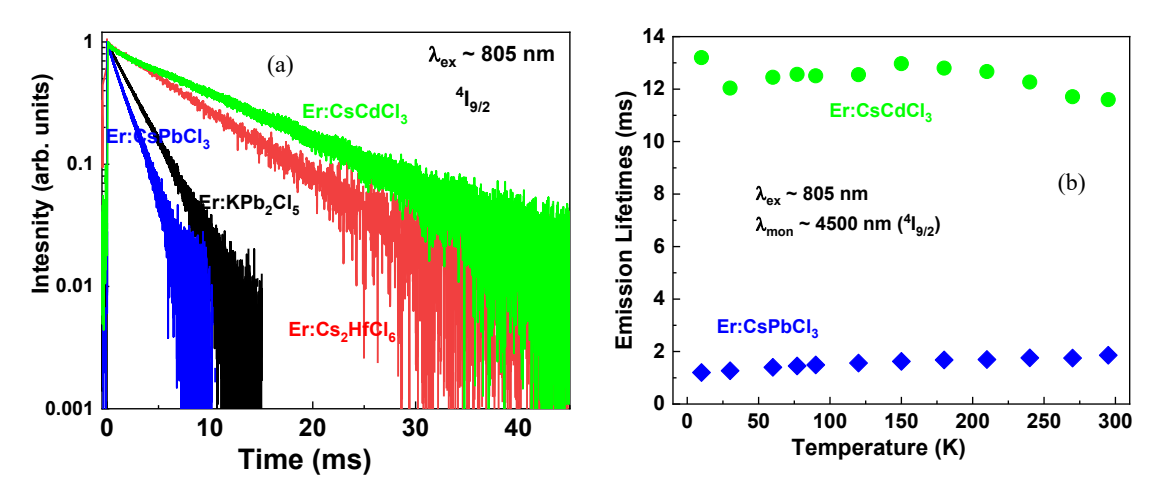


Figure 5. (a) Mid-IR emission decay transients of all studied Er^{3+} doped ternary chlorides monitored at 4500 nm ($^4I_{9/2} \rightarrow ^4I_{11/2}$) under 805 nm excitation at room temperature. (b) Temperature dependence of the $^4I_{9/2}$ level lifetime values between 10 K and room temperature for Er:CPC and Er:CPC arystals.

Table 3. Room temperature (experimental), radiative lifetimes, and quantum efficiencies of ${}^4I_{9/2} \rightarrow {}^4I_{11/2}$ transition for the investigated Er³⁺ doped KPC, CPC, and CCC crystals.

Crystal	τ _{300K} (ms)	τ _{rad} (ms)	η _{QE} (%)
Er:KPb2Cl5	3.2	3.9	~ 82
Er:CsPbCl ₃	1.85	1.85	~ 100
Er:CsCdCl3	11.6	13.0	~ 89

The stimulated emission cross-section of the ${}^4I_{9/2} \rightarrow {}^4I_{11/2}$ transition was calculated using the Füchtbauer-Landenburg equation [23]:

$$\sigma_{emiss}(\lambda) = \frac{\beta \lambda^5 I(\lambda)}{8\pi n^2 c \tau_{rad} \int \lambda I(\lambda) d\lambda}$$
 (2)

where β and τ_{rad} are the branching ratio of the 4500 nm emission and the radiative lifetime, respectively. $I(\lambda)$ is the emission intensity at wavelength λ and n is the refractive index of the host. The room temperature emission cross-section spectra of all Er doped chloride crystals is depicted in Fig. 6 (a), while Fig. 6 (b) displays the partial energy level diagram of Er³⁺ ions indicating the emission transition of interest ${}^{4}I_{9/2} \rightarrow {}^{4}I_{11/2}$. The peak emission cross-sections were determined to be $\sim 0.14 \times 10^{20}$ (@ 4400 nm), $\sim 0.54 \times 10^{20}$ (@ 4505 nm), and $\sim 0.14 \times 10^{20}$ (@ 4545 nm) cm² for Er:CHC, Er:CPC, and Er:CCC crystals, respectively. It was observed that the emission cross-sections for Er:CHC and Er:CCC are comparable to Er:KPC ($\sim 0.18 \times 10^{20}$ cm²) while the emission cross-section of Er:CPC is about three times higher than the Er:KPC value. The σ - τ product (where σ is the stimulated emission cross-section and τ is the upper laser level lifetime) is an important parameter to characterize laser materials since its value is inversely proportional to the laser threshold under continuous wave excitation. The larger the σ - τ product, the lower the threshold pump power. The σ - τ products of all four Er³⁺ doped chloride crystals along with other laser relevant parameters are summarized in Table 4. It is noted that the long lifetime leads to a large σ - τ product ($\sim 1.6 \times 10^{-20}$ cm².ms) for Er:CCC, which is over three times higher the values obtained for the Er:KPC crystal ($\sim 0.5 \times 10^{-20}$ cm².ms). These preliminary spectroscopic parameters for the studied Er³⁺ doped ternary chloride-based crystals compare favorably with other known IR laser transitions, which underlines the potential of these materials for solid-state laser applications at mid-IR wavelengths.

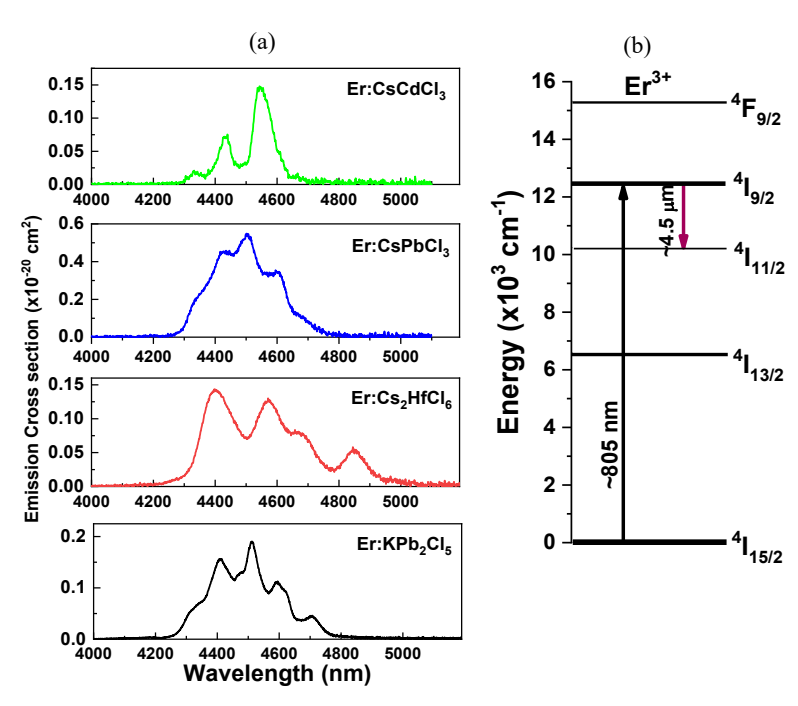


Figure 6. (a) Stimulated emission cross-section for the ${}^4I_{9/2} \rightarrow {}^4I_{11/2}$ transition in all investigated Er³⁺ doped ternary chlorides at room temperature, which were calculated using the Füchtbauer-Landenburg equation. (b) The partial energy level diagram of Er³⁺ ions indicating the emission transition of interest ${}^4I_{9/2} \rightarrow {}^4I_{11/2}$.

Table 4. Experimental lifetimes, calculated quantum yields, emission cross-sections, and sigma-tau product for the ${}^4I_{9/2}$ excited state for all studied four Er^{3+} doped ternary chloride crystals.

⁴ I _{9/2} → ⁴ I _{11/2}	Max. Phonon Energy (cm ⁻¹)	λ _{peak} (nm)	$ \begin{array}{c} $	$\sigma_{em}(\lambda)$ (10 ⁻²⁰ cm ²)	τ _{meas} (ms)	σ-τ (10 ⁻²⁰ cm ² .ms)
Er:KPb2Cl5	~ 203	~ 4510	~ 1.1 %	~ 0.18	3.2	~ 0.5
Er:Cs2HfCl6	~ 333	~ 4400		~ 0.14	7.8	~1.1
Er:CsPbCl ₃	~ 375	~ 4505	~ 1.3 %	~ 0.54	1.8	~ 0.97
Er:CsCdCl ₃	~ 252	~ 4545	~1.2 %	~ 0.14	11.6	~ 1.6

4. SUMMARY AND CONCLUSIONS

Initial results of a spectroscopic evaluation of Er^{3+} doped ternary-based chloride crystals, grown by Bridgman technique were presented. Mid-infrared fluorescence properties at room temperature, as well as at cryogenic temperatures, were explored. Broad mid-IR emission bands centered at ~4500 nm ($^4I_{9/2} \rightarrow ^4I_{11/2}$) were observed for all crystals under ~805 nm excitation. The room temperature fluorescence lifetimes for the $^4I_{9/2}$ manifold were measured to be ~7.8 ms, ~1.8 ms, and ~11.6 ms for Er^{3+} doped CHC, CPC, and CCC crystals, respectively. The peak mid-IR emission cross-sections at around 4500 nm for the studied crystals were determined to be between 0.14 - 0.54 x 10^{-20} cm². Based on the long

emission lifetime and the large σ - τ product values for the 4500 nm transition, the Er^{3+} doped CCC crystal appeared to be the most promising material among these studied chlorides for potential mid-IR lasers with low threshold operation. Nonetheless, a big factor in the applicability of these studied materials will be how well they can withstand the environmental conditions. For instance, Er^{3+} doped KPC has shown laser action in the mid-IR, it benefits from being non-hygroscopic, and it can be grown at good crystal quality. However, there is still some challenge growing this crystal at laser quality. As for Er^{3+} doped CHC, it displayed a long lifetime but it has limited usefulness due to hygroscopicity. While Er^{3+} doped CPC and CCC crystals showed some moisture sensitivity that could hamper laser operation, further material optimization and engineering is necessary to ensure that their material shortcomings do not detract from their spectroscopic potential.

ACKNOWLEDGEMENTS

The work at Hampton University was supported by the National Science Foundation through grant NSF-DMR 1827820 (PREM) and the Army Research Office through grant W911NF1810447. The work at Fisk University was supported by the Army Research Office through Contract No. W911NF1920278.

REFERENCES

- [1] Eichhorn, M., "Quasi-three-level solid-state lasers in the near and mid infrared based on trivalent rare earth ions," Appl Phys B. 93, 269-316 (2008).
- [2] Kaminskii, A.A., Crystalline lasers: physical processes and operating schemes. Boca Raton (FL): CRC Press (1996).
- [3] Velazquez, M., Ferrier, A., Doualan, J.-L. and Moncorge, R. "Rare-earth doped low phonon energy halide crystals for mid-infrared sources," in: A. Al-Khursan, editor. Solid-State Laser. London (UK): IntechOpen; pp. 119-142 (2012).
- [4] Bowman, S.R., Searles, S.K., Jenkins, N.W., Qadri, S.B., Skelton, E.F. and Ganem, J., "Diode pumped room temperature mid-infrared erbium laser," In: Marshall C, editor. Advanced Solid-State Lasers. Washington (DC): Optical Society of America; OSA trends in optics and photonics Vol. 50, 154–156 (2001).
- [5] Brown, E., Fleischman, Z., Merkle, L. D., Rowe, E., Burger, A., Payne, S. A. and Dubinskii M., "Optical spectroscopy of holmium doped K₂LaCl₅," J Lumin. 196, 221-226 (2018).
- [6] Orlovskii, Y.V., Basiev, T.T., Pukhov, K.K., Doroshenko, M.E., Badikov, V.V., Badikov, D.V., Alimov, O.K., Polyachenkova, M.V., Dmitruk, L.N., Osiko, V.V. and Mirov, S.B., "Mid-IR transitions of trivalent neodymium in low phonon laser crystals," Opt. Mater. 29, 1115-1128 (2007).
- [7] Okhrimchuk, A.G., Butvina, L.N., Dianov, E.M., Shestakova, I.A., Lichkova, N.V., Zagorodnev, V.N. and Shestakov, A.V., "Optical spectroscopy of the RbPb₂Cl₅:Dy³⁺ laser crystal and oscillation at 5.5 μm at room temperature," J. Opt. Soc. Am. B 24, 2690-2695 (2007).
- [8] Bowman, S.R., Shaw, L.B., Feldman, B.J. and Ganem, J., "A 7-µm praseodymium-based solid-state laser," IEEE J. Quantum Electron. 32, 646-649 (1996).
- [9] Brown, E., Hanley, C.B., Hommerich, U., Bluiett, A.G. and Trivedi, S.B. Trivedi, "Spectroscopic study of neodymium doped potassium lead bromide for mid-infrared solid state lasers," J. Lumin. 133, 244-248 (2013).
- [10] Jelinkova, H., Doroshenko, M.E., Jelinek, M., Sulc, J., Osiko, V.V., Badikov, V.V. and Badikov, D.V., "Dysprosium-doped PbGa₂S₄ laser generating at 4.3 μm directly pumped by 1.7 μm laser diode," Opt. Lett. 38, 3040-3043 (2013).
- [11] Nostrand, M.C., Page, R.H., Payne, S.A., Krupke, W.F. and Schunemann, P.G., "Room-temperature laser action at 4.3-4.4 µm in CaGa₂S₄:Dy³⁺," Opt. Lett. 24, 1215-1217 (1999).
- [12] Nostrand, M.C., Page, R.H., Payne, S.A., Schunemann, P.G. and Isaenko, L.I., "Laser demonstrations of rare-earth ions in low phonon chloride and sulfide crystals," in: H. Lasers, U. Injeyan, Keller, C. Marshall (Eds.), Advanced Solid State Lasers, OSA Topics in Optics and Photonics Series (Optical Society of America, Washington, D.C., Vol. 34, 459–463 (2000).
- [13] Calistru, D.M., Mihut, L., Lefrant, S. and Baltog, I., "Identification of the symmetry of phonon modes in CsPbCl₃ in phase IV by Raman and resonance-Raman scattering," J. Appl. Phys. 82, 5391-5395 (1997).

- [14] Demirbilek, R., Feile, R., and Bozdogan, C., "Temperature dependent Raman spectra of CsCdBr₃ and CsCdCl₃ crystals," J. Lumin. 161, 174-179 (2015).
- [15] Ariesanti, E., Hawrami, R., Burger, A. and Motakef, S., "Improved growth and scintillation properties of intrinsic, non-hygroscopic scintillator Cs₂HfCl₆," J. Lumin. 217, 116784 (1-5) (2020).
- [16] Kobayashi, M., Omata, K., Sugimoto, S., Tamagawa, Y., Kuroiwa, T., Asada, H., Takeuchi, T. and Kondo, S., "Scintillation characteristics of CsPbCl₃ single crystals," Nucl. Instrum. Methods Phys. Res., Sect. A 592(3), 369-373 (2008).
- [17] Romanov, A.N., Veber, A.A., Fattakhova, T., Vtyurina, D.N., Kouznetsov, M., Sulimov, V.B., "Spectral properties and NIR photoluminescence of Bi⁺ impurity in CsCdCl₃ ternary chloride," J. Lumin. 149, 292-296 (2014).
- [18] Virey, E., Couchaud, M., Faure, C., Ferrand, B. Wyon, C. and Borel, C., "Room temperature fluorescence of CsCdBr₃:RE (RE = Pr, Nd, Dy, Ho, Er, Tm) in the 3 5 µm range," J. Alloys Compd. 275-277, 311-314 (1998).
- [19] Hommerich, U., Uba, S., Kabir, A., Trivedi, S.B., Yang, C. and Brown, E., "Visible emission studies of melt-grown Dy-doped CsPbCl₃ and KPb₂Cl₅ crystals," Opt. Mater. Exp. 10(8), 2011-2018 (2020).
- [20] Lamichhane, A. and Ravindra, N., "Energy gap-refractive index relations in perovskites," Materials 13, 1917 (1-16), (2020).
- [21] Ghebouli, B., Ghebouli, M.A., Fatmi, M. and Bouhemadou, "First-principles study of the structural, elastic, electronic, optical and thermodynamic properties of the cubic perovskite CsCdCl₃ under high pressure," Solid St. Comm. 150, 1896-1901 (2010).
- [22] Jenkins, N.W., Bowman, S.B. Bowman, O'Connor, S., Searles, S.K. and Ganem, J., "Spectroscopic characterization of Er-doped KPb₂Cl₅ laser crystals," Opt. Mater. 22, 311-320 (2003).
- [23] Aull, B.F. and Jenssen, H.P., "Vibronic interactions in Nd:YAG resulting in nonreciprocity of absorption and stimulated emission cross sections," IEEE Quantum Electron. 18, 2559-2562 (2017).